Computational Toxicology 28 (2023) 100289

Contents lists available at ScienceDirect

Computational Toxicology

journal homepage: www.sciencedirect.com/journal/computational-toxicology

DFT study and docking of xanthone derivatives indicating their ability to inhibit aromatase, a crucial enzyme for the steroid biosynthesis pathway

Anamika Singh [a], Nikita Tiwari [b], Anil Mishra [b], Monika Gupta [a,*]

[a] Department of Chemistry, Babu Banarasi Das University, Lucknow, U.P. 2260 28, India
[b] Department of Chemistry, University of Lucknow, Lucknow, U.P. 2260 07, India

ARTICLE INFO

Keywords:
Xanthones
Aromatase
Breast cancer
Exemestane
Mulliken charges
Binding energy

ABSTRACT

Aromatase is a crucial enzyme in the aromatization process, which catalyzes the conversion of androgenic steroids to estrogens. Aromatase dysregulation, as well as elevated estrogen levels, have been linked to a variety of malignancies, including breast cancer. Herein, we present the results of the optimization of Xanthones employing density functional theory (DFT) using the B3LYP/6-311G+(d, p) basis set to determine their frontier molecular orbitals, Mulliken charges, and chemical reactivity descriptors. According to the DFT results, Erythrommone has the smallest HOMO-LUMO gap (3.85 Kcal/mol), as well as the greatest electrophilicity index (5.19) and basicity (4.47). Xanthones and their derivatives were docked into the active site cavity of CYP450 to examine their structure-based inhibitory effect. The docking simulation studies predicted that Erythrommone has the lowest binding energy (-7.43 Kcal/mol), which is consistent with the DFT calculations and may function as a powerful CYP450 inhibitor equivalent to its known inhibitor, Exemestane, which has a binding affinity of −8.13 Kcal/mol. The high binding affinity of Xanthones was linked to the existence of hydrogen bonds as well as various hydrophobic interactions between the ligand and the receptor's essential amino acid residues. The findings demonstrated that Xanthones are more powerful inhibitors of the Aromatase enzyme than the recognized inhibitor Exemestane.

1. Introduction

Aromatase is a member of the cytochrome P450 superfamily of enzymes. It is a membrane-bound protein that is localized in the endoplasmic reticulum. The human aromatase (CYP450) is located in the genome. Aromatase (also known as estrogen synthetase or estrogen synthase) is the key enzyme involved in the catalysis of androgenic steroids to estrogens through the aromatization process as in Fig. 1. Estrogenic steroid hormones play a vital role in many key physiological processes including growth, oessification, differentiation, neurologic and reproductive development hence, the enzyme is expressed in diverse tissues, including skin, endometrium, bone, brain, ovary, testis, placenta, mammary and adipose tissue. The maintenance of estrogen levels is dynamic and is dependent on reproductive age [1]. In premenopausal women, 17β-estradiol, the most potent estrogen synthesized in the ovaries, acts as a circulating hormone and exerts its effect on distant target organs in an endocrine fashion. However, in postmenopausal women, upon cessation of ovarian function, circulating estrogens decrease and estrogens are synthesized predominantly in adipose tissues and other extra-gonadal tissues such as brain, bone, breast, and skin which have the machinery to metabolize available androgen substrates [1].

Dysregulation of aromatase, as well as increased levels of estrogen, has been implicated in many cancers including breast cancers [2,3,4].

This has led to the use of aromatase inhibitors (AIs) in the clinic for the treatment of estrogen-dependent breast cancers due to their improved therapeutic effect over estrogen modulator, tamoxifen, in post-menopausal women [6,7].

Exemestane is a 17-oxo steroid, a selective inhibitor of the aromatase (estrogen synthase) system, it is used in the treatment of advanced breast cancer. Exemestane decreases bone mineral density when it is used for a long period and low bone mineral density finally causes weak bones or osteoporosis. Serious adverse effects of Exemestane include Cough or hoarseness, difficulty or labored breathing, fever or chills, lower back or side pain, mental depression, swelling of the hands, ankles, feet, or lower legs, tightness in the chest are all symptoms to watch out for [8,9,10].

In this research, we find that the need for a novel selective Aromatase inhibitor with fewer side effects is growing, and a more effective and

* Corresponding author.
E-mail address: monika.gupta@bbdu.ac.in (M. Gupta).

https://doi.org/10.1016/j.comtox.2023.100289
Received 13 June 2023; Received in revised form 16 September 2023; Accepted 26 September 2023
Available online 28 September 2023

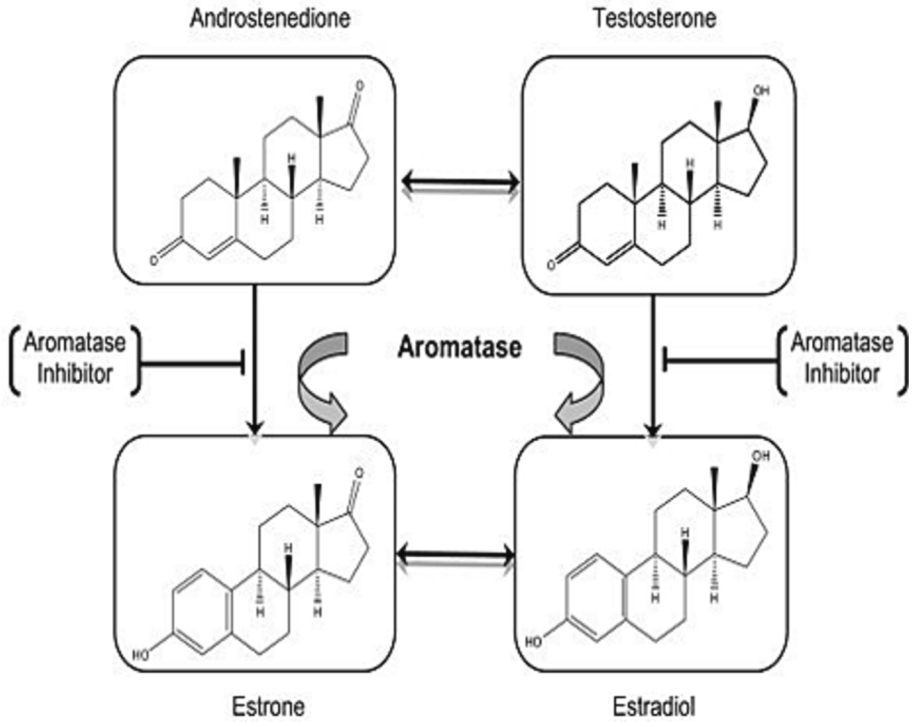

Fig. 1. Schematic diagram of the reaction catalyzed by the aromatase enzyme [5] (Image source Khan et al 2011) (W640.jpg).

quick drug discovery approach is needed. Using molecular docking is a technique to research a new medicine that is both more effective and efficient.

This study focuses on the critical interactions of Xanthones with human placental aromatase cytochrome P450 (CYP19A1), which ultimately inhibits CYP19A1 activity. It is now possible to view the crystal structure of human placental aromatase complexed with the breast cancer medication Exemestane (PDB ID: 3S7S). Exemestane, a known aromatase inhibitor [11,12], interacts at the active site of CYP19A1 and forms hydrophobic bonds with Arg115, Ile133, and Cys437.

In silico and virtual models provide a promising option for improving understanding of the impact of various substances on physiological processes and chemico-biological interactions. Xanthones are an example of a broad set of chemical entities that have garnered attention in the modern period of pharmacology.

The binding mechanism and stability of these Xanthones to human CYP19A1 were investigated using molecular docking and DFT experiments. Molecular docking studies allow for the prediction of a possible molecular interaction of these ligands with enzymes from diverse pathways that lead to the creation of important molecules [13]. The following nine common Xanthones were employed in this work for docking investigations with CYP19A1: Demethylchodatin, Erythrommone, Lichexanthone, Norlichexanthone, Griseoxanthone, and Thiophaninic Acid, Gentisein, Norathyriol and Mangiferin.

DFT simulations were utilized to determine the molecular structure with the lowest energy, molecular orbitals, Mulliken charges, and chemical reactivity characteristics. These characteristics are important in describing the amount of the Xanthones interaction in the CYP19A1 binding pocket. The xanthone's lowest HOMO-LUMO gap describes how an inhibitor's HOMO can transfer electrons to lower energy, LUMO of amino acid residues in an enzyme's active site. These xanthones were chosen because they are common phytochemicals that are freely accessible. The findings indicate that these xanthones can bind and inhibit the activity of CYP19A1. As a result, xanthone binding to CYP19A1 alters the basal androgen to estrogen ratio, which in turn impacts the steroid production pathway.

2. Materials and methods

2.1. DFT calculations

Computational calculations were implemented by using density functional theory (DFT) [14] with the hybrid functional B3LYP [14,15,16] by using a 6-311G+(d, p) basis set in the gas phase in the Gaussian09 program package [17,18,19].The study starts with the optimization of the geometry of all the xanthones and then the optimized geometrical parameters are used in the calculation of the energy of HOMO (Highest Occupied Molecular Orbital), LUMO (Lowest Unoccupied Molecular Orbital), energy gap (ΔE), dipole moment (μ) and free energy.

2.2. Molecular docking

The interaction of xanthones with CYP19A1 was investigated using computational docking techniques. The docking of xanthones with CYP19A1 was carried out using AutoDock 4.2.6 [20]. AutoDock calculates the binding free energy of a small molecule to a macromolecule using a semi empirical free energy force field. The coordinates of CYP19A1 were obtained from the RCSB database from the crystal structure of human placental aromatase complexed with the breast cancer drug Exemestane (PDB ID: 3S7S). By deleting heteroatoms, as well as adding explicit hydrogen molecules and corresponding Kollman

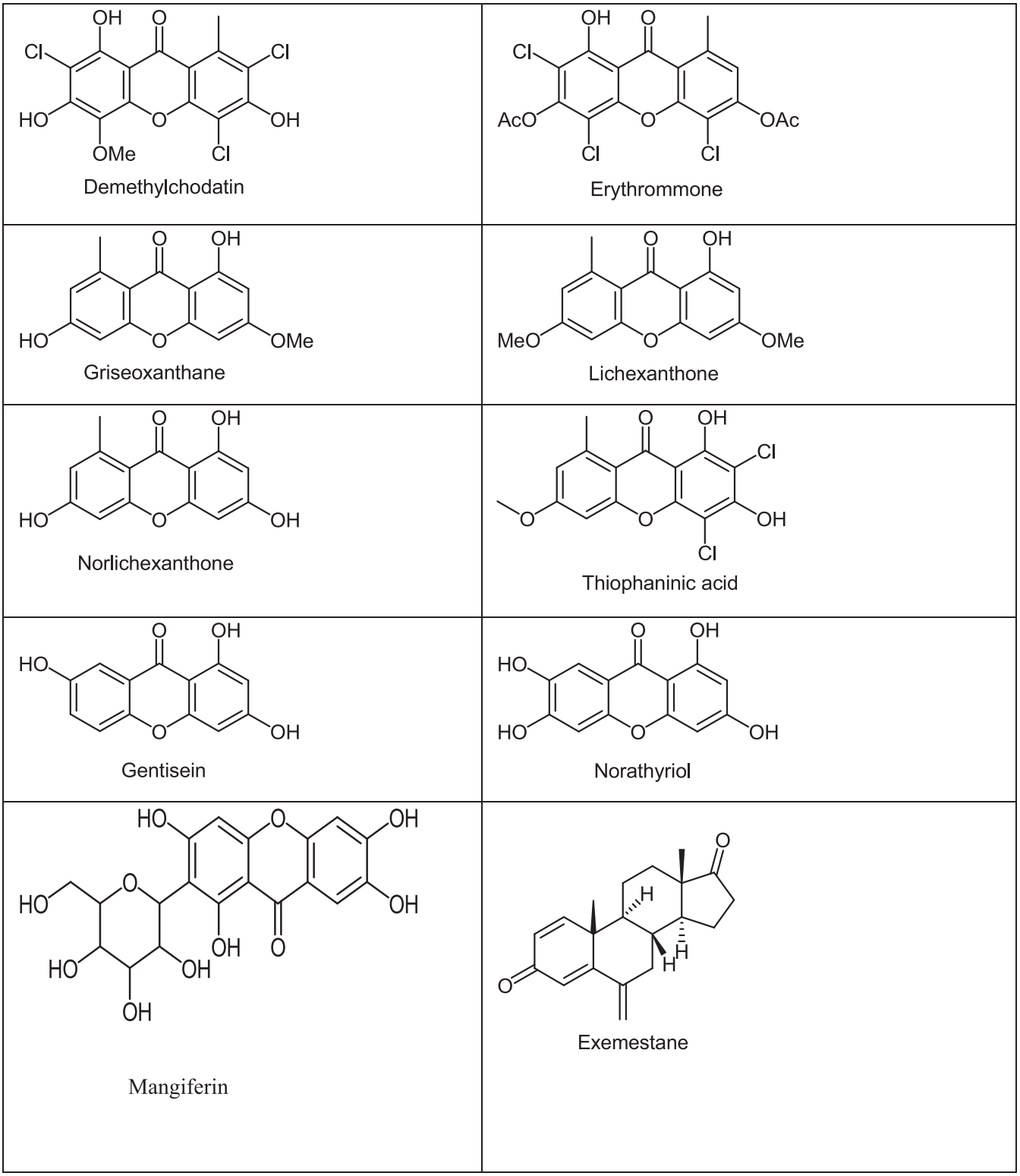

Fig. 2. 2D Structures of Xanthones.

charges (16.0), a receptor molecule was created and saved in.pdbqtfile format. Demethylchodatin, Erythrommone, Lichexanthone, Norlichexanthone, Griseoxanthone, and Thiophaninic Acid, Gentisein, Norathyriol, and Mangiferin are nine common xanthones used in docking studies with CYP19A1. Exemestane, a known inhibitor of CYP19A1, was docked as a positive control and its binding affinity scores with xanthones were compared. Gauss View 5.0 was used to create the 3D structures of all the xanthones. The ligands were created by combining hydrogen atoms and Gasteiger charges before being saved in.pdbqt format. The torsional degrees of freedom of a ligand molecule were specified using ligand flexibility. The Lamarckian genetic algorithm and the grid-supported energy evaluation method were used for docking. The pose with the highest binding affinity score and the associated interactions were chosen and visually viewed and analyzed in LigPlot.

Demethylchodatin 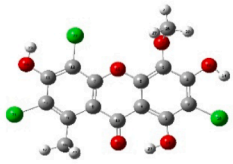	Erythrommone 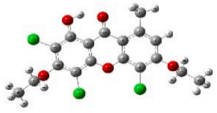
Griseoxanthone 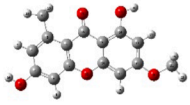	Lichexanthone 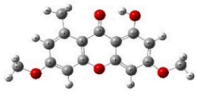
Norlichexanthone 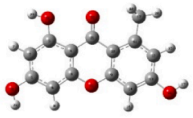	Thiophaninic Acid 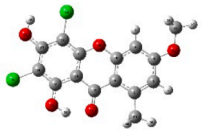
Gentisein 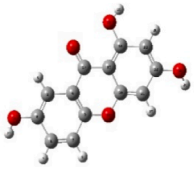	Norathyriol 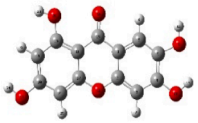
Mangiferin 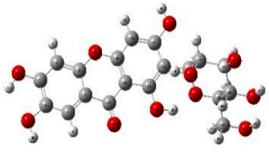	Exemestane 

Fig. 3. 3D STRUCTURES OF XANTHONES.

Table 1
HOMO, LUMO, gap, hardness (η), softness (δ), electronegativity (χ), electrophilicity index (ω), ionization potential (I) and electron affinity (A) of all the compounds.

Ligand	HOMO	LUMO	ΔE	χ	η	δ	ω	I.P	E.A
Demethylchodatin	**6.4061**	**2.4446**	**3.96**	**4.42**	**1.98**	**0.50**	**4.94**	**6.40**	**2.44**
Erythrommone	**6.4023**	**2.5480**	**3.85**	**4.47**	**1.92**	**0.51**	**5.19**	**6.40**	**2.54**
Griseoxanthone	**6.2186**	**1.5744**	**4.64**	**3.89**	**2.32**	**0.43**	**3.26**	**6.21**	**1.57**
Lichexanthone	**6.1415**	**1.8860**	**4.25**	**4.01**	**2.12**	**0.46**	**3.78**	**6.14**	**1.88**
Norlichexanthone	**6.3569**	**1.6209**	**4.73**	**3.98**	**2.36**	**0.42**	**3.35**	**6.35**	**1.62**
Thiophaninic Acid	**6.3852**	**2.2259**	**4.15**	**4.30**	**2.07**	**0.48**	**4.45**	**6.38**	**2.22**
Norathyriol	**6.1389**	**1.7589**	**4.37**	**3.94**	**2.18**	**0.45**	**3.56**	**6.13**	**1.75**
Gentisein	**6.1536**	**1.9170**	**4.23**	**4.03**	**2.11**	**0.47**	**3.84**	**6.15**	**1.91**
Mangiferin	**6.2442**	**1.8680**	**4.38**	**4.05**	**2.19**	**0.46**	**3.74**	**6.24**	**1.86**
Exemestane	**6.8058**	**2.1543**	**4.65**	**4.48**	**2.32**	**0.42**	**4.31**	**6.80**	**2.15**

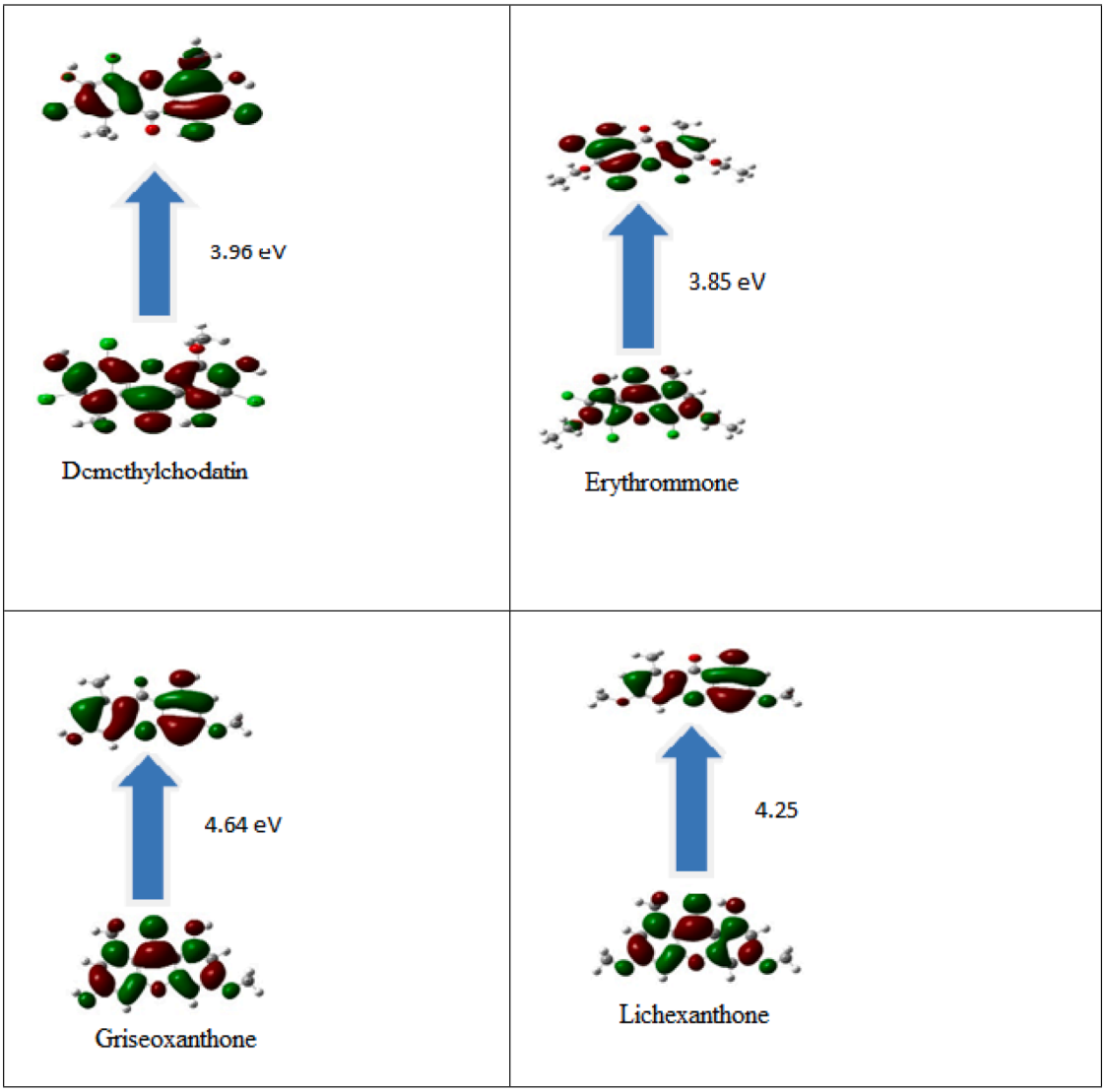

Fig. 4. HOMO-LUMO Gap in the Xanthones and Exemestane.

3. Results and discussion

3.1. DFT calculation studies

The theoretical DFT calculations were carried out using the Gaussian09 software on the basis set B3LYP 6-311G+(d,p). The structural geometry was optimized by minimizing its energy in comparison to all geometrical variables while avoiding any molecular symmetry constraints. GaussView 5.0 [21] was used to depict the molecular structure of the optimizedxanthones as can be seen in Fig. 2and Fig. 3.

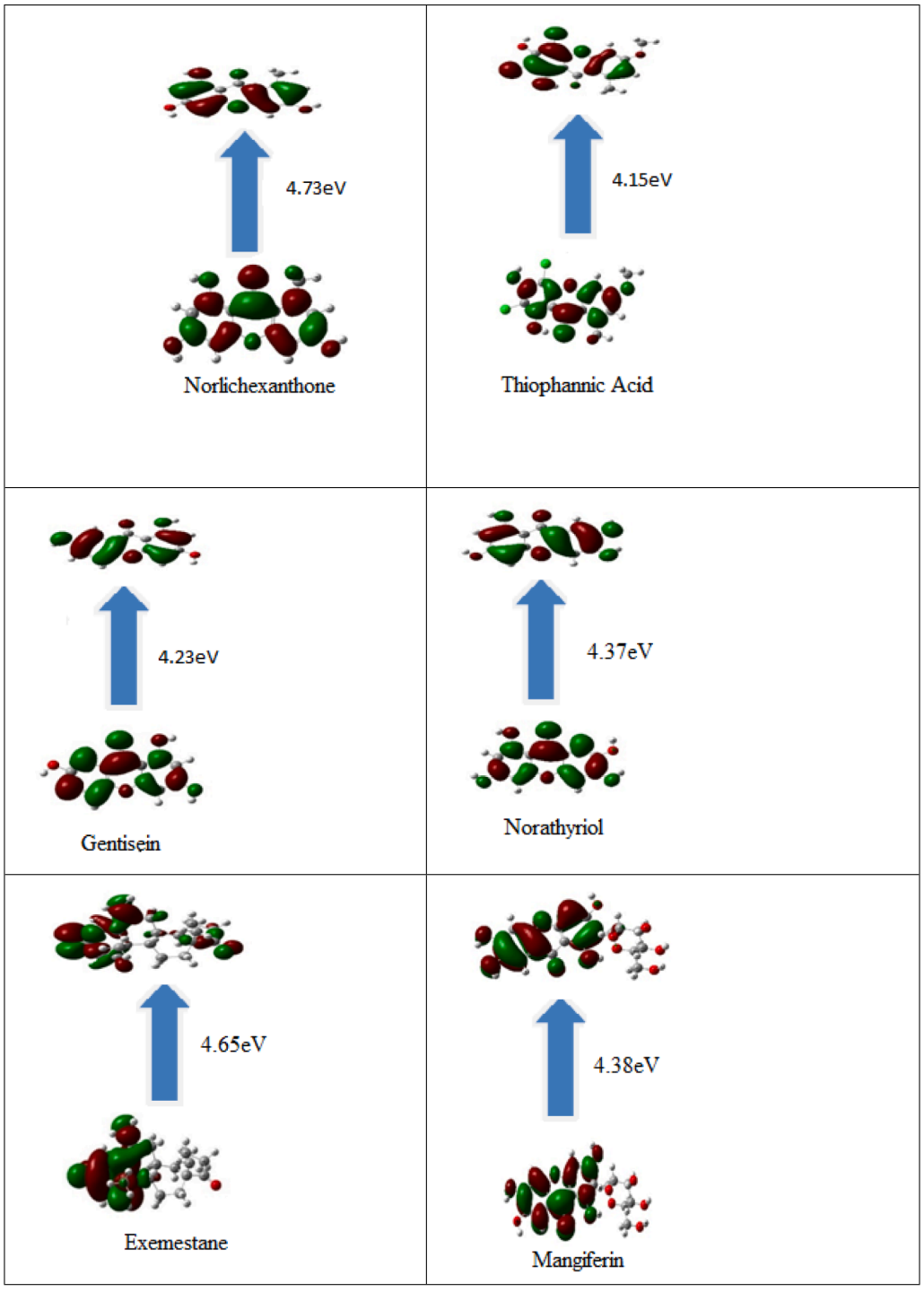

Fig. 4. (*continued*).

Table 2
Mulliken charges of the corresponding Xanthones.

Demethylchodatin		Erythrommone		Griseoxanthane		Lichexanthone		Norlichexanthone		Thiophannic Acid		Norathyriol		Gentisein		Mangiferin	
1C	−0.945	1C	−0.924	1C	−0.199	1C	−1.001	1C	−0.656	1C	0.931	1C	1.430	1C	0.199	1C	−0.217
2C	1.509	2C	0.212	2C	0.955	2C	−0.043	2C	0.326	2C	−0.344	2C	−0.967	2C	−0.154	2C	−0.228
3C	−0.346	3C	−0.285	3C	0.986	3C	0.005	3C	0.358	3C	−0.665	3C	−0.053	3C	−1.127	3C	−0.767
4C	−0.138	4C	0.808	4C	0.038	4C	0.963	4C	1.427	4C	0.014	4C	−0.274	4C	1.492	4C	1.594
5C	0.209	5C	0.587	5C	−0.218	5C	0.796	5C	−1.051	5C	0.156	5C	−0.153	5C	0.250	5C	0.091
6C	−1.002	6C	−0.152	6C	−0.628	6C	0.050	6C	−0.293	6C	0.901	6C	0.329	6C	−0.330	6C	−0.106
7C	−0.053	8C	−0.314	9C	1.677	9C	−0.969	9C	−0.280	9C	−0.077	9C	−0.061	10C	−1.154	9C	−0.844
8C	0.404	9C	−0.216	10C	−0.056	10C	−0.242	10C	0.797	10C	0.282	10C	0.024	11C	−0.228	10C	−0.705
9C	0.476	10C	−1.642	11C	0.243	11C	−0.986	11C	0.915	11C	1.112	11O	−0.286	12C	−0.611	11C	−0.443
10C	0.844	11C	1.081	12C	−0.816	12C	0.540	12C	−0.069	12C	0.254	12O	−0.035	12C	0.210	12C	0.410
11C	−1.984	12C	−0.085	13C	−0.179	13C	−0.116	13C	−0.602	13C	−1.657	15C	0.093	13C	0.161	13C	0.191
12C	0.541	13C	0.260	14C	−1.294	14C	1.506	14C	−0.039	14C	1.579	16C	1.414	14C	1.349	14C	1.038
13C	−0.464	14C	−0.162	17Cl	0.040	17C	−0.322	17C	0.108	15C	−0.770	17C	−1.156	17C	0.150	16C	0.366
14O	0.076	15O	0.116	18O	0.207	18O	−0.034	18O	−0.787	16O	−0.172	18C	0.225	18O	−0.001	17C	−0.006
15O	−0.331	16O	−0.331	19O	−0.271	19O	−0.357	19O	−0.258	17O	−0.331	19C	0.144	19O	−0.042	18C	−0.128
16O	0.077	17Cl	0.260	20O	−0.035	20O	−0.172	20O	−0.029	18O	0.042	20C	−0.650	20O	0.017	19C	0.118
17O	−0.170	18Cl	0.264	21O	0.022	21O	−0.169	21O	0.022	19O	0.139	21C	−0.132	21O	0.092	20C	0.043
18O	0.075	19Cl	0.341	22O	0.097	22O	0.027	22O	0.096	20O	0.090	26O	0.087	22O	−0.272	25C	−0.412
19O	0.167	20O	−0.055	23C	−0.172	23C	0.113	23C	0.016	21C	0.214	27O	0.021			26O	−0.046
20Cl	0.326	21O	0.094	27C	−0.399	27C	0.204	27C		25C	0.068					27O -	−0.276
21Cl	0.378	22O	0.008	31C		31C	0.208	31C		29Cl	0.161					28O	0.028
22Cl	0.189	24C	0.078							30Cl	0.298					29O	−0.052
26C	0.154	28C	0.043													30O	0.143
30C	0.006	32C	0.019													31O	0.053
		36C	0.001													32O	−0.006
		37C	−0.006													33O	−0.045
																39O	−0.022
																41C	0.270
																42O	−0.021

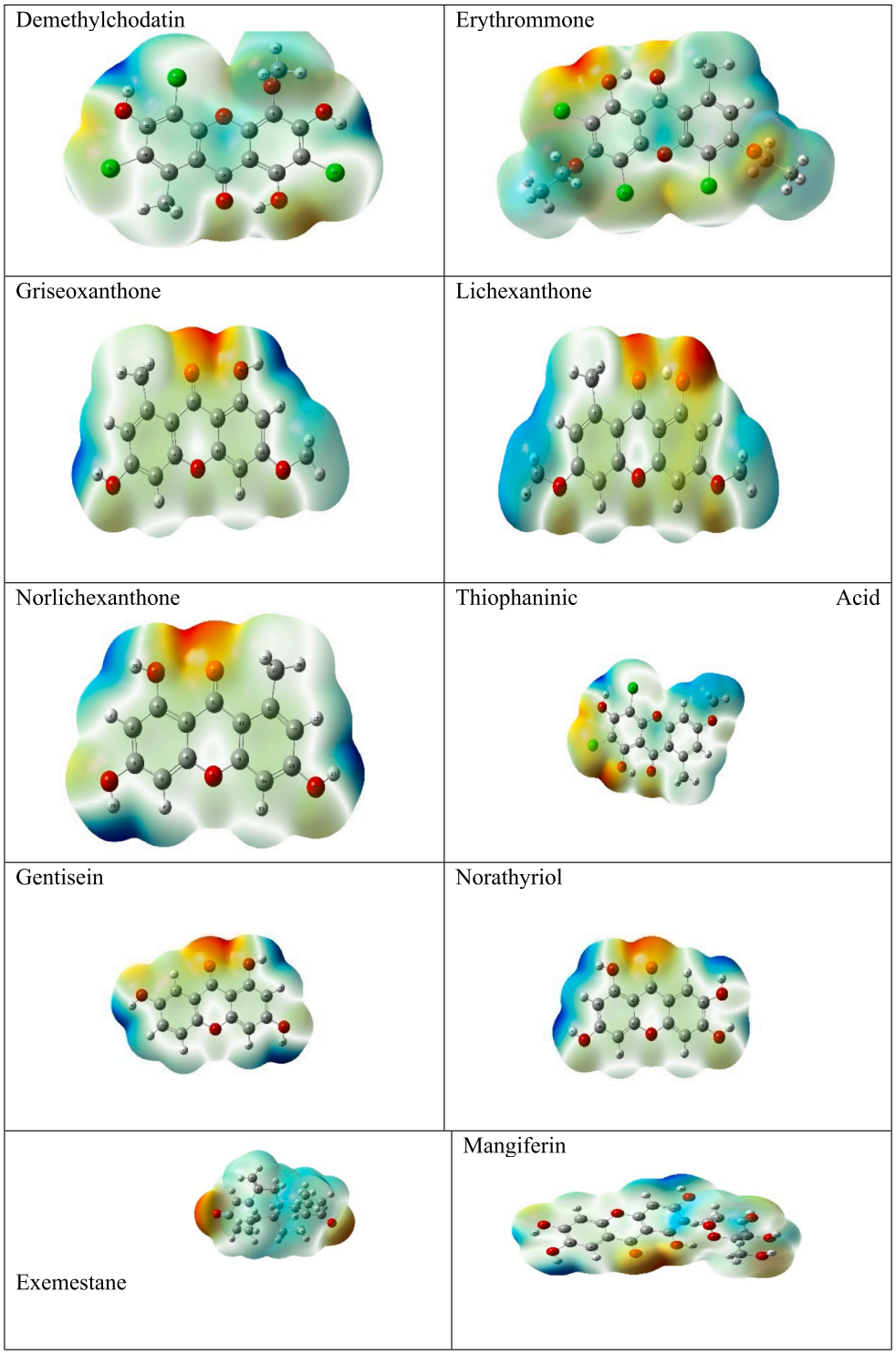

Fig. 5. MEP in the Xanthones.

3.2. *Frontier molecular orbitals*

Frontier molecular orbitals (FMOs) are the highest occupied molecular orbital (HOMO) with electrons, making it an electron donor, and the lowest unoccupied molecular orbital (LUMO) with an electron acceptor space. Both are critical quantum chemical parameters for calculating a variety of key factors such as chemical reactivity descriptors. Table 1 summarises all of the calculations.

Table 3
Binding affinity of all the studied Xanthones and known Inhibitor Exemestane.

Ligands	Binding Energy(kcal/mol)
Demethylchodatin	−6.03
Erythrommone	−7.43
Griseoxanthone	−6.42
Lichexanthone	−6.27
Norlichexanthone	−6.19
Thiophaninic Acid	−6.24
Gentisein	−5.52
Norathyriol	−4.50
Mangiferin	−2.73
Exemestane	−8.13

Fig. 4 depicts the isodensity surface plots of HOMO and LUMO for the analyzedxanthones.

In this study, Erythrommone has the smallest HOMO-LUMO gap of 3.85 eV among xanthones, while Norlichexanthone has the biggest energy gap of 4.73 eV. A large HOMO-LUMO gap is associated with high kinetic stability and low chemical reactivity, whereas a small HOMO-LUMO gap is associated with low chemical stability, because electron addition to a high-lying LUMO and/or electron removal from a low-lying HOMO is energetically advantageous in any potential reaction.

3.3. Chemical reactivity descriptors

The energies of frontier HOMOs and LUMOs were also used to compute the chemical reactivity descriptors hardness (η), softness(δ), electronegativity(χ), and electrophilicity index (ω) of all xanthones using the Parr and Pearson interpretation of DFT [22,23] and the Koopmans theorem [24].

The following equations are used for the calculation of hardness (η), electronegativity (χ), and softness (δ) [25, 26]:

$$\eta = -1/2(\mathrm{EHOMO} - \mathrm{ELUMO}) \quad (1)$$

$$\chi = -1/2(\mathrm{EHOMO} + \mathrm{ELUMO}) \quad (2)$$

$$\delta = 1/\eta \quad (3)$$

$$\omega = \chi^2/2\eta \quad (4)$$

The value ofelectronegativity (χ) indicates a Lewis acid, while tiny values of electronegativity specify an excellent base,which is a molecule's ability to attract electrons.Global softness(δ) refers to a molecule's capacity to accept electrons while global hardness(η) refers to the degree to which charge transfer is prohibited.Soft molecules are more reactive than harder ones because they can transport electrons to acceptors more readily, whereas hardness (η) relates to the extent to which charge transfer is blocked. It combined LYP (Lee, Yang, and Parr) correlation function with Becke (B) exchange functional B3LYP (25, 26).Amongst Xanthones, Erythrommone showed higher basicity (χ = 4.47) and highest electrophilicity index (ω = 5.19).

3.4. Mulliken charges

The Mulliken atomic charges of the estimated Xanthonescalculated by the DFT were tabulated in Table 2.

The study of Mulliken charges demonstrated that the greatest positive charges for Erythrommone are C11 and 15O, respectively. On the other hand, it has been found that the most electrophilic susceptibility sites of Erythrommone are 16O and C10.However, the compounds' most negatively charged cores are those that are most likely to act as electrophilic sites as shown in the Fig. 5.

3.5. Molecular docking

Molecular docking is a popular computational method for validating the interaction of an appropriate orientation of a small molecule with a receptor protein. The findings of this study revealed that because the benzene rings of Xanthones are structurally similar to the known inhibitor, Exemestane, they are likely to imitate the binding mechanism at the active site of CYP19A1 as shown in Fig. 5.

Table. 3 depicts thatxanthones have binding energies ranging from 6.03 to 7.43 kcal/mol,

which is comparable to exemestane (8.13 kcal/mol). These xanthones occupied the active site cavity, which included residues like Arg115, Ile133, Phe134, Asp306, Val370, Leu372, Leu477, and Ser478, in the same way as Exemestane (Fig. 6).

Nonbonding interactions, in addition to regular hydrogen bonding, are often used terms to describe the form and behaviour of molecules. These Xanthones also formed polar H-bonds as in Table 4.

These findings imply that all of the Xanthones investigated can bind to the active site of CYP19A1. Furthermore, Erythrommone appears to be a powerful CYP19A1 inhibitor.

As demonstrated in Table 3, Xanthones have binding energies ranging from 6.03 to 7.43 kcal/mol, which is comparable to exemestane (8.13 kcal/mol). These Xanthones occupied the active site cavity, which included residues like Arg115,Val373,Ile133,Cys437,Leu477, Val370, Phe134,Pro429,Phe430 and Leu372 in the same way as Exemestane (see Fig. 6). Nonbonding interactions, in addition to regular hydrogen bonding, are often used terms to describe the form and behavior of molecules. These Xanthones also formed polar H-bonds with the amino acid residue Met374(2.71A) of cytochrome *P*-450 as in Table 4). These findings imply that all of the Xanthones investigated can bind to the active site of CYP19A1 exactly as in the case of the popular inhibitor Exemestane. Furthermore, Erythrommone appears to be a powerful CYP19A1 inhibitor.

The negative Mulliken charges on oxygen atoms in xanthones, as previously mentioned from DFT simulations, could be taken advantage for hydrogen bond interactions with protein receptors. HOMOs have energy levels ranging from −6.13 eV to −6.41 eV, whereas LUMOs have energy levels ranging from −1.62 eV to −2.54 eV, depending on conjugation and the presence of polar groups. Furthermore, Erythrommone's low FMO energy gap (E = 3.85), high basicity (χ = 4.47) and high electrophilicity index (ω = 5.19) compared to others may have an effect on binding affinity. Furthermore, docking experiments revealed that Erythrommone binds to aromatase with the lowest binding energy (-7.43 kcal/mol), supporting the DFT investigations. All of these elements may interact to varying degrees to greatly influence the degree of binding affinity of these xanthones.

4. Conclusion

Aromatase (also known as estrogen synthetase or estrogen synthase) is the key enzyme involved in the catalysis of androgenic steroids to estrogens through the aromatization process. Dysregulation of aromatase as well as increased levels of estrogen has been implicated in many cancers including breast cancers The inhibition of CYP19A1 activity is used in the treatment of advanced breast cancer. Xanthones are the naturally available phytochemicals, have been investigated as inhibitors for aromatase by DFT and molecular docking calculations.According to this computational analysis, complexes like Xanthone-CYP450 have

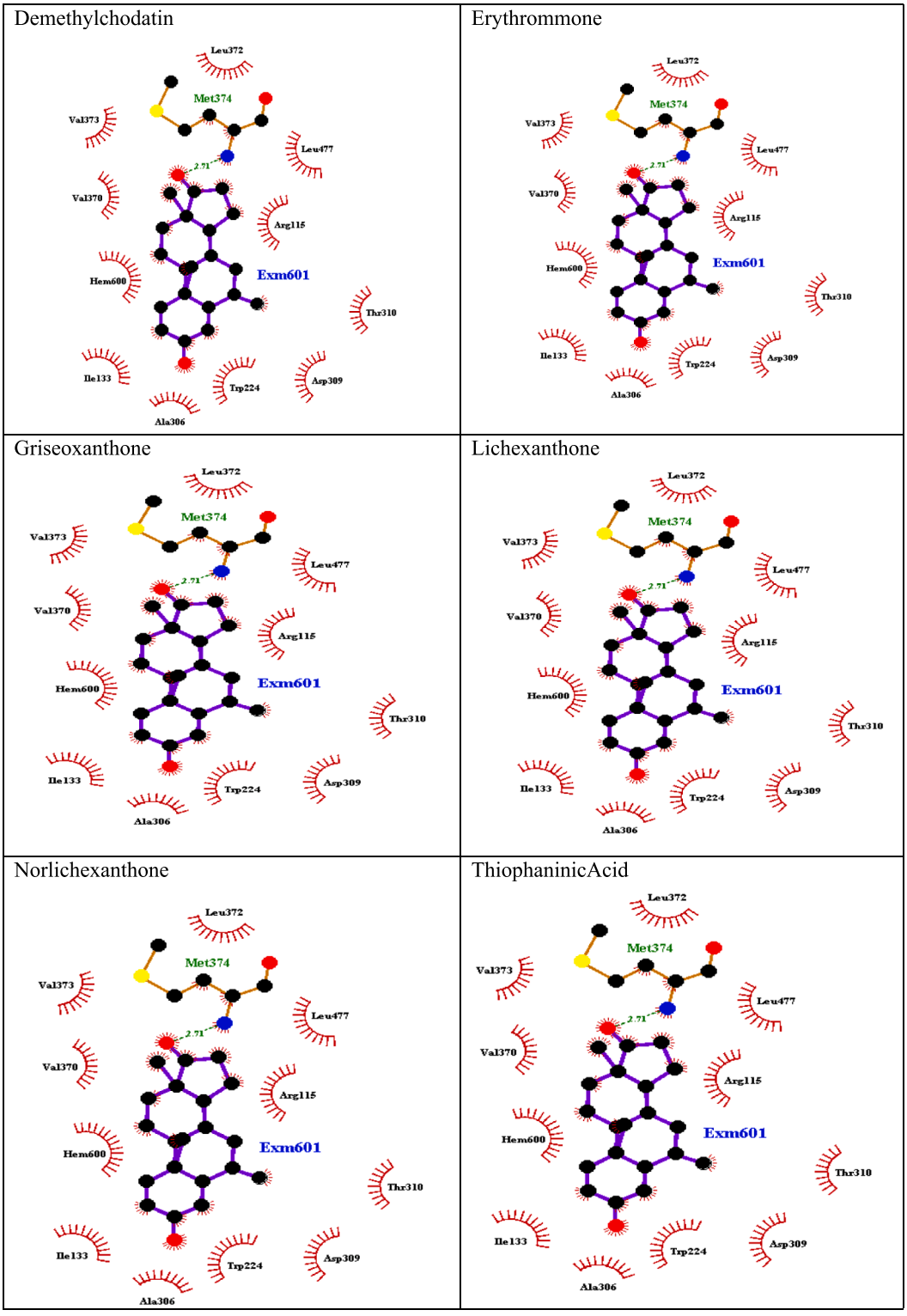

Fig. 6. Amino acid residues in the protein binding pocket.

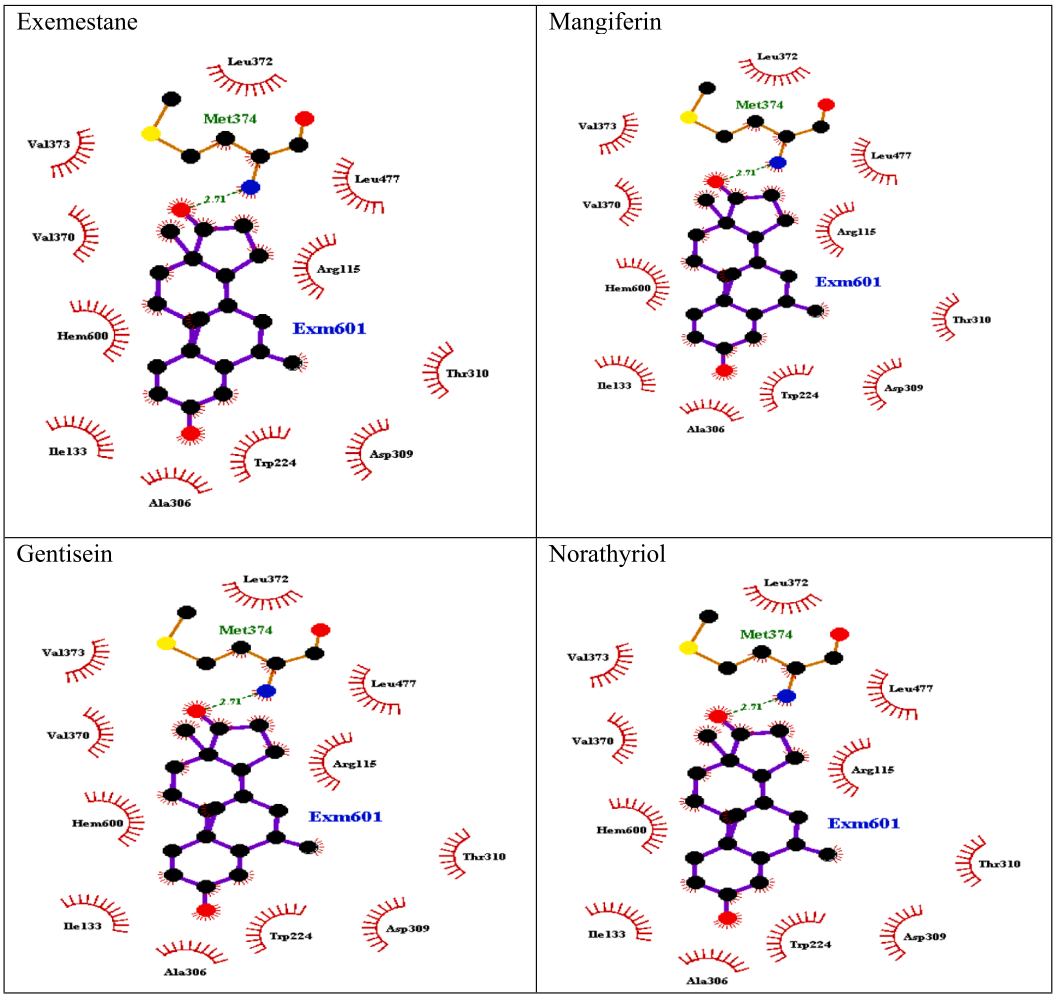

Fig. 6. (*continued*).

Table 4
Amino acid residues in the Aromatase(3S7S) binding pocket.

Ligand	Type of interactions		Number of bonds	
	H-bond residues	Hydrophobic bond residues	H-bonds	Hydrophobic bonds
Demethylchodatin	Met374 (2.71 Å)	Arg115,Val373,Ile133,Cys437,Leu477 Val370,Phe134,Pro429,Phe430,Leu372	1	10
Erythrommone	Met374 (2.71 Å)	Arg115,Val373,Ile133,Cys437,Leu477 Val370,Phe134,Pro429,Phe430,Leu372	1	10
Griseoxanthone	Met374 (2.71 Å)	Arg115,Val373,Ile133,Cys437,Leu477 Val370,Phe134,Pro429,Phe430,Leu372	1	10
Lichexanthone	Met374 (2.71 Å)	Arg115,Val373,Ile133,Cys437,Leu477 Val370,Phe134,Pro429,Phe430,Leu372	1	10
Norlichexanthone	Met374 (2.71 Å)	Arg115,Val373,Ile133,Cys437,Leu477 Val370,Phe134,Pro429,Phe430,Leu372	1	10
Thiophaninic Acid	Met374 (2.71 Å)	Arg115,Val373,Ile133,Cys437,Leu477 Val370,Phe134,Pro429,Phe430,Leu372	1	10
Exemestane	Met374 (2.71 Å)	Arg115,Val373,Ile133,Cys437,Leu477 Val370,Phe134,Pro429,Phe430,Leu372	1	10
Gentisein	Met374 (2.71 Å)	Arg115,Val373,Ile133, Cys437,Leu477 Val370,Phe134,Pro429,Phe430,Leu372	1	10
Norathyriol	Met374 (2.71 Å)	Arg115,Val373,Ile133, Cys437,Leu477 Val370,Phe134,Pro429,Phe430,Leu372	1	10
Mangiferin	Met374 (2.71 Å)	Arg115,Val373,Ile133,Leu477,Trp224 Val370,Asp309,Thr310,Leu372,Hem600	1	10

binding affinities similar to those of known inhibitor-protein complexes like Exemestane-CYP450. Xanthones can effectively bind to CYP450 and block it from acting along the pathway of steroid production to achieve this. As there are numerous medications or treatments used as inhibitors in fatal diseases like breast cancer, each has advantages and disadvantages of its own. After investigating using density functional theory and

docking, we discovered Erythrommone, a derivative of readily available xanthone phytochemicals, as a safe aromatase inhibitor.This study also provides a major technique in the identification of novel and effective anticancer compounds from xanthone derivatives, and it can be used as a reference for future studies for screening and creating structurally varied compounds from the xanthone family.

Declaration of Competing Interest

The authors declare the following financial interests/personal relationships which may be considered as potential competing interests: MONIKA GUPTA reports administrative support was provided by Babu Banarasi Das University.

Data availability

Data will be made available on request.

References

[1] E.R. Simpson, Role of aromatase in sex steroid action, J. Mol. Endocrinol. 25 (2) (2000) 149–156.
[2] S. Manna, M.K. Holz, Tamoxifen action in ER-negative breast cancer, Signal Transduction Insights 5 (2016) STI-S29901.
[3] H. Zahid, E.R. Simpson, K.A. Brown, Inflammation, dysregulated metabolism and aromatase in obesity and breast cancer, Curr. Opin. Pharmacol. 31 (2016) 90–96.
[4] R.J. Santen, C.A. Stuenkel, W. Yue, Mechanistic effects of estrogens on breast cancer, The Cancer Journal 28 (3) (2022) 224–240.
[5] S.I. Khan, J. Zhao, I.A. Khan, L.A. Walker, A.K. Dasmahapatra, Potential utility of natural products as regulators of breast cancer-associated aromatase promoters, Reprod. Biol. Endocrinol. 9 (1) (2011) 1–10.
[6] R. Carpenter, W.R. Miller, Role of aromatase inhibitors in breast cancer, Br. J. Cancer 93 (1) (2005) S1–S5.
[7] J.A. Ligibel, E.P. Winer, Aromatase inhibitors as adjuvant therapy for postmenopausal women: a therapeutic advance but many unresolved questions, Breast Cancer Res. 7 (2005) 1–3.
[8] X. Qian, Z. Li, GuoDong Ruan, C. Tu, W.u. Ding, Efficacy and toxicity of extended aromatase inhibitors after adjuvant aromatase inhibitors-containing therapy for hormone-receptor-positive breast cancer: a literature-based meta-analysis of randomized trials, Breast Cancer Res. Treat. 179 (2) (2020) 275–285.
[9] H. Wildiers, N.A. de Glas, Anticancer drugs are not well tolerated in all older patients with cancer, The Lancet Healthy Longevity 1 (1) (2020) e43–e47.
[10] (https://www.mayoclinic.org/drugs-supplements/end-user-acknowledgement).
[11] R.B. Tan, A.T. Guay, W.J. Hellstrom, Clinical use of aromatase inhibitors in adult males, Sexual Medicine Reviews 2 (2) (2014) 79–90.
[12] D.I. Shulman, G.L. Francis, M.R. Palmert, E.A. Eugster, Use of aromatase inhibitors in children and adolescents with disorders of growth and adolescent development, Pediatrics 121 (4) (2008) e975–e983.
[13] A. le Maire, W. Bourguet, P. Balaguer, A structural view of nuclear hormone receptor: endocrine disruptor interactions, Cell. Mol. Life Sci. 67 (8) (2010) 1219–1237.
[14] M.P. Gleeson, D. Gleeson, QM/MM calculations in drug discovery: a useful method for studying binding phenomena? J. Chem. Inf. Model. 49 (3) (2009) 670–677.
[15] A.D. Becke, Density-functional exchange-energy approximation with correct asymptotic behavior, Phys. Rev. A 38 (6) (1988) 3098–3100.
[16] C. Lee, W. Yang, R.G. Parr, Development of the Colle-Salvetti correlation-energy formula into a functional of the electron density, Phys. Rev. B 37 (2) (1988) 785–789.
[17] Frisch, M. J. (2009) Guassian 09, Gaussian, Wallingford, CT, There is no corresponding record for this reference.
[18] H. Kruse, L. Goerigk, S. Grimme, Why the standard B3LYP/6-31G* model chemistry should not be used in DFT calculations of molecular thermochemistry: understanding and correcting the problem, J. Org. Chem. 77 (23) (2012) 10824–10834.
[19] Parr, R. G. (1980). Density functional theory of atoms and molecules. In Horizons of Quantum Chemistry: Proceedings of the Third International Congress of Quantum Chemistry Held at Kyoto, Japan, October 29-November 3, 1979 (pp. 5-15). Springer Netherlands.
[20] G.M. Morris, R. Huey, W. Lindstrom, M.F. Sanner, R.K. Belew, D.S. Goodsell, A. J. Olson, AutoDock4 and AutoDockTools4: Automated docking with selective receptor flexibility, J. Comput. Chem. 30 (16) (2009) 2785–2791.
[21] Dennington, R., Keith, T., &Millam, J. (2009). Semichem Inc. Shawnee Mission KS, GaussView, Version, 5(8).
[22] R.G. Pearson, The HSAB principle—more quantitative aspects, InorganicaChimicaActa 240 (1–2) (1995) 93–98.
[23] R.G. Pearson, Absolute electronegativity and hardness correlated with molecular orbital theory, Proc. Natl. Acad. Sci. 83 (22) (1986) 8440–8441.
[24] N. Tiwari, A. Kumar, A. Pandey, A. Mishra, Computational investigation of dioxin-like compounds as human sex hormone-binding globulin inhibitors: DFT calculations, docking study and molecular dynamics simulations, Comput. Toxicol. 21 (2022), 100198.
[25] N. Tiwari, A. Pandey, A. Kumar, A. Mishra, Computational models reveal the potential of polycyclic aromatic hydrocarbons to inhibit aromatase, an important enzyme of the steroid biosynthesis pathway, Comput. Toxicol. 19 (2021), 100176.